Arab J Sci Eng (2015) 40:1027–1044
DOI 10.1007/s13369-015-1591-3

RESEARCH ARTICLE - CIVIL ENGINEERING

Structural Damage Identification Using Response Surface-Based Multi-objective Optimization: A Comparative Study

Tanmoy Mukhopadhyay · Tushar Kanti Dey · Rajib Chowdhury · Anupam Chakrabarti

Received: 28 October 2014 / Accepted: 19 January 2015 / Published online: 6 February 2015

Abstract Non-destructive structural damage identification (SDI) and quantification of damage are important issues for any engineering structure. In this study, a comparative assessment of the damage identification capability of different design of experiment (DOE) methods (such as, 2^k factorial design, central composite design, Box–Behnken design, D-optimal design and Taguchi's OA design) used in response surface methodology (RSM) has been carried out. Three different structures (simply supported beam, spring mass damper system and fibre reinforced polymer composite bridge deck) have been used for various single and multiple damage conditions to access the comparative ability of the aforementioned methods in identifying damage addressing two critically important criteria: accuracy and computational efficiency. The study reveals that central composite design and D-optimal design are most recommendable among the five considered DOE methods for SDI. Two different input parameter screening methods (sensitivity analysis using RSM utilizing 2^k factorial design and D-optimal design, general sensitivity analysis) have been explored in this study, and their comparative performance is also discussed. It is found that both the methods used in sensitivity analysis for the purpose of input parameter screening in the damage identification process work satisfactorily. Performance of RSM-based damage identification algorithm for different DOE methods under the influence of noise has also been addressed in this paper.

T. Mukhopadhyay (✉)
College of Engineering, Swansea University, Swansea, UK
e-mail: tanmoym.89@gmail.com

T. K. Dey · R. Chowdhury · A. Chakrabarti
Department of Civil Engineering, Indian Institute of Technology Roorkee, Roorkee, India

Keywords Non-destructive structural damage identification · Response surface methodology · Design of experiments · Sensitivity analysis · Multi-objective optimization

1 Introduction

Damage in structures is defined by the changes to the material and/or geometric properties of the systems, including changes to the boundary conditions and system connectivity, which adversely affect the system's performance [1]. Identification of damage in an existing structure is very important to ensure the conditions of safety and serviceability. Numerous methods have been developed so far for damage detection in structures [2–9]. These methods can be broadly classified as global techniques and local techniques. Further, both dynamic and static measures can be adopted for damage identification. In global dynamic techniques, the structure is usually subjected to low-frequency excitations of the order 4–100 Hz. The fundamental idea behind vibration-based damage identification techniques is—the damage-induced changes in the physical properties (such as mass, damping and stiffness) will cause detectable changes in modal properties (such as natural frequencies, modal damping and mode shapes) of the structure. So the damage can be identified by analysing the changes in vibration features of the structure. Several global vibration-based algorithms have been proposed in last two decades to locate and quantify damages in simple structures, such as the change in natural frequency method [10], the change in curvature mode shape method [11], the change in stiffness method [12], the change in flexibility method [13] and the damage index method [14]. Application of global static techniques such as the static displace-

ment response technique [15] and static strain measurement technique [16] for damage identification has also been explored. Local damage identification techniques rely on localized exploration of structures, and these methods are best to use when approximate damage location is known a priori. Different techniques under this category are ultrasonic wave propagation, acoustic emission, eddy currents, impact echo testing, magnetic field methods, electrical methods, dye penetrate testing and X-ray radiograph [17,18]. Of late, electro-mechanical impedance (EMI) technique [19,20] and wavelet-based approach [21–26] have been proposed for damage identification. Advantage of these methods is that no prior information about the responses of undamaged structure is needed. Another most promising recently proposed global dynamic damage identification technique is based on response surface method (RSM), which is gaining rapid popularity because of its computational efficiency. A concise literature survey on this technique is presented in the next paragraph.

Response surface-based damage identification algorithm relies on model updating technique, which is based on the modification of structural model matrices (such as mass, stiffness, and damping) to reproduce as closely as possible to the measured dynamic response of the actual damaged structure. Comparisons of the updated matrices to the initial matrices provide an indication of damage and can be used to quantify the location and extent of damage [27,28]. In response surface-based model updating techniques, the actual finite element model is replaced by a response surface metamodel, making the process very much computationally efficient and cost-effective. SDI using RSM involves formation of response surface equation and inverse optimization to achieve some target value of the responses with the help of different statistical and mathematical techniques. RSM was primarily proposed by Box and Wilson [29] for application in chemical industry. After that, the methodology has been modified and enriched rigorously for achieving different objectives. Comprehensive description about RSM can be found in [30,31]. RSM has been widely applied in many fields of science and technology over time [32–40]. But the state of application of RSM in structural dynamics problems or particularly in damage identification problems is still very scarce. Some of the applications of RSM in structural dynamics related problems can be found in [41–44]. Cundy [45] gave a preliminary idea of using RSM in damage detection of structures. Cho [46] performed an investigation using RSM to predict the accumulated damages in concrete structures. Fang and Perera [47] established a comprehensive methodology for damage identification using RSM. Casciati [48] used linear response surface models for representing the relationship between samples of response time histories to identify damage in structure. The main attractive feature of RSM-based damage identification technique is its computational efficiency and the ability to quantify damage along with identifying damage location.

Though previous studies reveal that RSM-based method has the potential to be successfully applied in structural damage identification, at the same time, these researches initiate the need to explore the method further. One of the most interesting scopes of research in the present context that still remains to be addressed is to explore comparative ability of different DOE methods of RSM in SDI. This investigation will enable future researchers to choose the appropriate DOE method for SDI from the viewpoint of accuracy as well as computational efficiency. The present work aims to provide a detail comparative study on the capability of different design methods of RSM (such as, 2^k factorial design, central composite design, Box–Behnken design, D-optimal design and Taguchi's OA design) in damage identification. Another important aspect that needs attention is the performance of RSM-based SDI under the influence of noise, which is inevitable in practical situation. The present research investigates this aspect as well, considering different DOE methods. This paper is organized as, Sect. 1: introduction, Sect. 2: brief overview of different design methods of RSM, Sect. 3: different steps of SDI based on RSM algorithm, Sect. 4: discussion on the comparative capability of different DOE methods in SDI with the help of three illustrative numerical models, Sect. 5: Performance of different DOE methods in RSM-based damage identification methods under the effect of noise, and Sect. 6: conclusion.

2 Response Surface Methodology

On the basis of statistical and mathematical analysis, RSM gives an approximate equation, which relates the input features ξ and output features y for a particular system.

$$y = f(\xi_1, \xi_2, \ldots, \xi_k) + \varepsilon \tag{1}$$

where f denotes the approximate response function and ε is the statistical error term having a normal distribution with mean zero. k is the number of input parameters. The input features ξ are usually coded as dimensionless variables having mean zero and the same standard deviation of ξ. The commonly used first-order and second-order polynomials are of following shapes.

First-order model (interaction):

$$y = \beta_0 + \sum_{i=1}^{k} \beta_i x_i + \sum_{i=1}^{k} \sum_{j>i}^{k} \beta_{ij} x_i x_j + \varepsilon$$

Second-order model:

$$y = \beta_0 + \sum_{i=1}^{k} \beta_i x_i + \sum_{i=1}^{k} \sum_{j>i}^{k} \beta_{ij} x_i x_j + \sum_{i=1}^{k} \beta_{ii} x_i^2 + \varepsilon \tag{2}$$

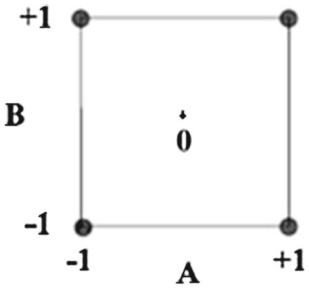

Fig. 1 2^k fractional design for two factors

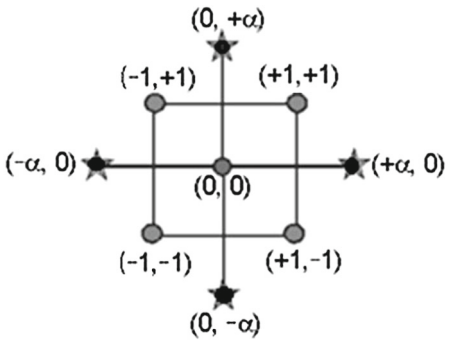

Fig. 2 Two factor Central composite design

The metamodel is fit approximately to a set of points in the design space (which may be chosen using design of experiment approach) using a multiple regression fitting scheme. Design of experiments (DOEs) is an efficient procedure for planning experiments so that the data obtained can be utilized to achieve any particular goal. The commonly used DOE methods for constructing response surface models are described below.

2.1 2^k Factorial Design

One of the most common first-order designs is 2^k factorial design (2^k FD), which is very useful for screening out some non-significant input parameters by determining the contribution of each parameter to the total model variance. In this design, every input parameter has two coded levels (± 1), that correspond to the lower and upper value bound of the design space as shown in Fig. 1. For example, in case of a simple beam, if the upper and lower limits of Young's modulus (E) and section moment of inertia (I) are 28, 32 GPa and 2.278×10^{-4} m^4, 3.255×10^{-4} m^4, respectively, then the coded values for E and I can be obtained by simple linear transformation as

$$\text{coded value of E} = \frac{\text{Actual value of } E - 30}{2} \tag{3}$$

$$\text{coded value of I} = \frac{\text{Actual value of } I - 2.7665 \times 10^{-4}}{0.4885 \times 10^{-4}} \tag{4}$$

In this design, the number of experimental runs is equal to 2^k provided no single design point is replicated more than once. If k is large ($k \geq 5$), the 2^k design requires a large number of design points. In that case, we can consider a one-half fraction design consisting of one-half the number of points of a 2^k design, or a one-fourth fraction design consisting of one- fourth the number of points of a 2^k design. In general, a 2^{-m}th fraction of a 2^k design consists of 2^{k-m} points from a full 2^k design. m should be chosen in such a way that $2^{k-m} \geq$ number of unknowns in the response surface equation. Sometimes, a few additional centre point samples (level = 0) are added to the design to evaluate the curvature of the middle region of the design space [30,31].

2.2 Central Composite Design

Central composite design (CCD) is the most popular second-order design, which consists of the following three portions: a complete (or a fraction of) 2^k factorial design coded as ± 1, $2k$ axial points coded as $\pm\alpha$ ($\alpha \geq 1$) and n_0 centre points (generally 5 or 6) as shown in Fig. 2. Augmentation of the design by additional α actually extends the bound of the design space. Thus, the total number of design points in a CCD is $n = 2^k + 2k + n_0$. If $k = 10$ and $n_0 = 6$, then total number of design points required is $n = 2^{10} + 2 \times 10 + 6 = 1{,}050$, which needs considerable amount of computational effort. So, instead of complete design, a fractional CCD (1/2, 1/4 or 1/8 and a minimum run with resolution V (MRRV) fractions requiring 538, 282, 154 and 82 samples, respectively, for $k = 10$ and $n_0 = 6$) may be adopted. The values of α and n_0 are chosen in such a way so that the CCD possesses certain desirable properties, and according to the value of α, CCD can be rotatable (used for up to 5 factors, this creates a design that has the standard error of predictions equal at points equidistant from the centre of the design), face-centred (this puts the axial points into the faces of the cube at ± 1 levels. This produces a design where each factor only has 3 levels), spherical (this puts all factorial and axial points on the surface of a sphere of radius equal to square root of the number of factors), orthogonal quadratic (provides alpha values that allow the quadratic terms to be independently estimated from the other terms), and practical (used for 6 or more factors. The alpha value is the fourth root of the number of factors) [30,31].

2.3 Box–Behnken Design

Box–Behnken design (BBD) is another popular second-order rotatable design. It provides three levels (-1, 0, 1) for each factor and consists of a particular subset of 3^k factorial design

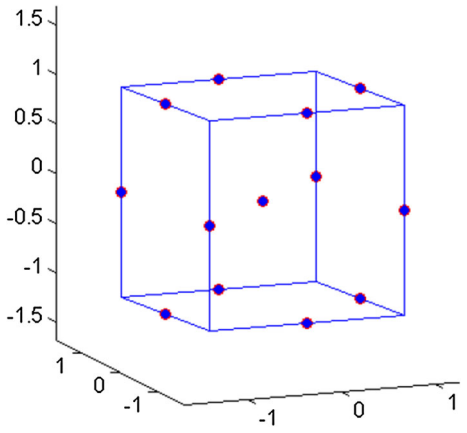

Fig. 3 Box–Behnken (BB) design for 3 factors

as shown in Fig. 3. BBD provides good result near centre of the design space but weaker at the corner of the cube, i.e. for extreme values of the input factors [30,31].

2.4 Optimal Design

Optimal designs require fewer samples than the other standard design procedures, and thus, it is much more computationally feasible mainly in case of large number of input factors. In this design, position of design points is chosen algorithmically according to the number of factors, and the desired model and the points are not at any specific positions, they are selected to meet the optimality criteria. Optimal designs can be used to create a good design for fitting a linear, quadratic, cubic or higher-order models. There are several types of optimality criteria such as D-optimality, A-optimality and E-optimality. D-optimality is achieved if the determinant of $(X^{\mathrm{t}}X)^{-1}$ is minimal. A-optimality is achieved by minimizing the trace of $(X^{\mathrm{t}}X)^{-1}$. E-optimality is achieved if the largest eigenvalue of $(X^{\mathrm{t}}X)^{-1}$ is minimal. Here, X denotes the design matrix as a set of value combinations of coded parameters, and X^{t} is the transpose of X [30,31,49]. In D-optimal design, the total sample size (n) comprises of minimum design points (n_{d}), additional model points ($n_a = k$) and lack-of-fit points (n_{l}). (i.e. $n = n_{\mathrm{d}} + n_{\mathrm{a}} + n_{\mathrm{l}}$). Required model points (i.e. minimum design points) are the minimum number of runs to estimate the coefficients for the terms in the design for model, while additional model points are extra runs added by the user to improve precision estimates or coverage of the factor space, and lack-of-fit points are the extra points to fill the factor space. The extra information provided by these points can test the fit of the model. For model construction in the present study, an over-determined D-optimal design [33,50,51] (number of additional samples n_{a}, along with the minimum point design and $n_{\mathrm{l}} = 5$ samples to estimate the lack of fit) has been used.

2.5 Taguchi's OA Design

Taguchi designs are a type of factorial design. Design options are available with differing numbers of parameters and levels. In Taguchi's orthogonal array design, the interaction between different parameters is not considered explicitly, and thus, this design method works best for discrete variables. Taguchi developed a system of tabulated designs, which reduce the number of experiments considerably as compared to a full factorial design [30,31].

After selection of the design points using DOE method as discussed above, a response surface metamodel (as shown in Eq. 2) is constructed using the method of least squares. Method of least squares is a multiple regression technique, and it is assumed in this method that random errors are identically distributed with a zero mean and a common unknown variance, and they are independent of each other. The difference between the observed (y) and the fitted value ($\overline{y_i}$) for the ith observation $\varepsilon_i = y_i - \overline{y_i}$ is called the residual. Criterion for choosing the β_i estimates of equation $y = X\beta + \varepsilon$ (refer Eq. 2) is that they should minimize the sum of the squares of the residuals, which is often called the sum of squares of the errors (SSEs). Thus,

$$\mathrm{SSE} = \sum_{i=1}^{n} \varepsilon_i^2 = \sum (y_i - \overline{y_i})^2 \tag{5}$$

The residuals may be written as

$$\varepsilon = y - X\beta \tag{6}$$

The SSE thus becomes

$$\mathrm{SSE} = \varepsilon^{\mathrm{T}}\varepsilon = (y - X\beta)^{\mathrm{T}}(y - X\beta) \tag{7}$$

Differentiating the SSE with respect to β using partial derivatives and equating it to zero, one can get $X\beta = y$. This over-determined system of equations can be solved directly to obtain the coefficients β as follows

$$\beta = (X^{\mathrm{T}}X)^{-1}X^{\mathrm{T}}y \tag{8}$$

After obtaining the coefficients β as described above, response surface metamodel can be easily constructed. The major drawback of RSM is to fit the design points to a second-order polynomial as systems having high degree of nonlinearity cannot be replaced by a second-order model. To overcome this lacuna, the data can be converted into another form using suitable transformation scheme to capture the higher-degree nonlinearity. For example, using logarithmic transformation or power transformation, the response surface model takes the following forms:

$$\ln y = \beta_0 + \sum_{i=1}^{k} \beta_i x_i + \sum_{i=1}^{k} \sum_{j>i}^{k} \beta_{ij} x_i x_j + \sum_{i=1}^{k} \beta_{ii} x_i^2 + \varepsilon$$

$$y^n = \beta_0 + \sum_{i=1}^{k} \beta_i x_i + \sum_{i=1}^{k} \sum_{j>i}^{k} \beta_{ij} x_i x_j + \sum_{i=1}^{k} \beta_{ii} x_i^2 + \varepsilon \tag{9}$$

Quality of a response surface model should be checked following several criteria before using it as discussed in Sect. 3.3.1.

3 Damage Identification Based on RSM

Damage detection using RSM is a four step procedure: step-1: Identification of structure of interest, step-2: Identification of proper input and output features, step-3: Formation of response surface relating input and output features, step-4: Identification of damage, as shown in Fig. 4. This section contains detailed description about SDI using RSM.

3.1 Identification of Structure of Interest

First step of SDI is to identify the structure whose damage is needed to be identified. In this study, three different structures have been taken: simply supported beam, five Degrees of freedom system consisting of spring, mass, damper and a fibre reinforced polymer (FRP) composite bridge deck.

3.2 Identification of Proper Input and Output Features

Material properties, such as Young's modulus, density, Poisson's ratio and geometric properties such as section inertia, may be taken as input parameters depending on the type of structure under consideration. Time domain features (peak acceleration, temporal moments, logarithmic decrement, etc.) and frequency domain features (such as, modal frequencies, mode shapes.) are generally taken as output. For highly nonlinear structures, time domain features are more suitable than frequency domain features. Selected output features should not be highly correlated with each other, and they should be sensitive enough to the chosen input features.

If the effects of the modelling errors in the baseline finite element model exceed the modal sensitivity to damage, accurate damage estimation may not be possible to carry out [6]. Although updating the modal baseline using the measured data from the original model may improve estimation accuracy, it is not always practically feasible for most of the real-life structures, since a lot of measurement information would be required. For this reason, output features should be chosen in such a way so that they are least sensitive possible to the modelling errors in the baseline finite element model and the most sensitive possible to damage. This problem can be solved by studying the free vibration equations for undamaged and damaged structures as described below.

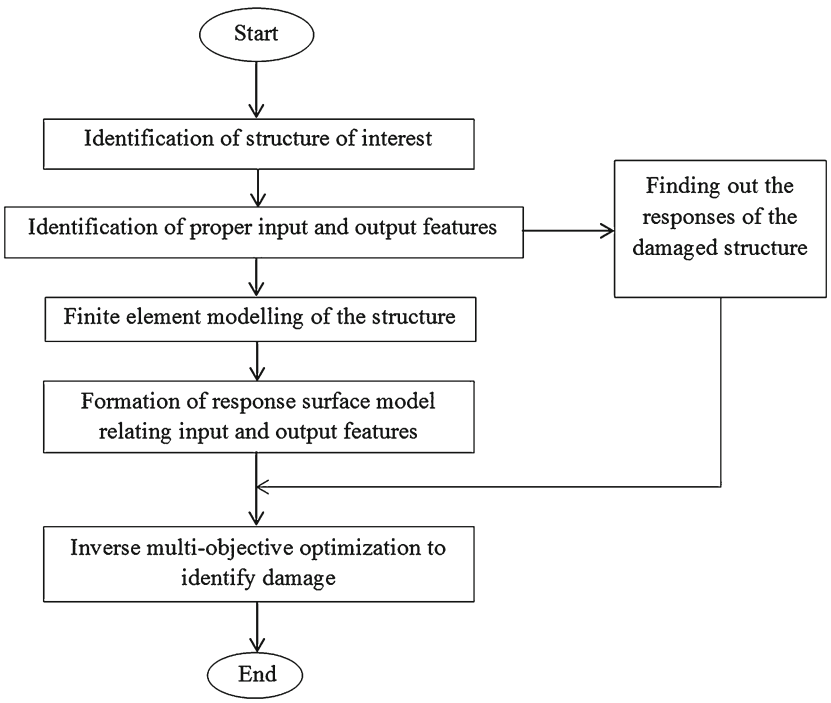

Fig. 4 Flowchart of the RSM-based damage identification algorithm

In the case of no modelling errors,

$$([K]-\lambda_j[M])\{\phi_j\}=0, \quad j=1,\ldots N_m \tag{10}$$

$$\left(([K]+\Delta[K])-\left(\lambda_j+\Delta\lambda_j^{\mathrm{d}}\right)[M]\right)\left(\{\phi_j\}+\Delta\{\phi_j^{\mathrm{d}}\}\right)=0 \tag{11}$$

In the case of existing modelling errors of value $\Delta[\bar{K}]$ in the baseline model,

$$\left(([K]+\Delta[\bar{K}])-(\lambda_j+\Delta\bar{\lambda}_j)[M]\right)\left(\{\phi_j\}+\Delta\{\bar{\phi}_j\}\right)=0 \tag{12}$$

$$\left(([K]+\Delta[K]+\Delta[\bar{K}])-\left(\lambda_j+\Delta\bar{\lambda}_j^{\mathrm{d}}+\Delta\bar{\lambda}_j\right)[M]\right)\left(\{\phi_j\}+\{\Delta\bar{\phi}_j^{\mathrm{d}}\}+\Delta\left\{\bar{\phi}_j\right\}\right)=0 \tag{13}$$

where $[K]$, $[M]$ and N_{m} are the global stiffness matrix, mass matrix and the total number of mode shapes considered, respectively. λ_j is the square of the natural frequency corresponding to vibration mode $\{\phi_j\}$. In this study, damage has been modelled as reduction in stiffness $\Delta[K]$. This change in stiffness leads to a change in square of frequencies $\Delta\lambda_j^{\mathrm{d}}$ and mode shapes $\Delta\{\phi_j^{\mathrm{d}}\}$. The symbol $(\bar{\cdot})$ indicates the modal quantities involving errors. By neglecting higher-order terms of Δ in the above expressions and pre-multiplying by $\{\phi_j\}^{\mathrm{T}}$, we get

$$\Delta\lambda_j^{\mathrm{d}}=\Delta\bar{\lambda}_j^{\mathrm{d}}\approx\frac{\{\phi_j\}^{\mathrm{T}}\Delta[K]\{\phi_j\}}{\{\phi_j\}^{\mathrm{T}}[M]\{\phi_j\}} \tag{14}$$

Again from Eqs. (11), (13) and (14), we can obtain

$$([K]-\lambda_j[M])\left(\Delta\left\{\phi_j^{\mathrm{d}}\right\}-\Delta\left\{\bar{\phi}_j^{\mathrm{d}}\right\}\right)\approx 0 \tag{15}$$

Equation (15) leads to

$$\left(\Delta\left\{\phi_j^{\mathrm{d}}\right\}-\Delta\left\{\bar{\phi}_j^{\mathrm{d}}\right\}\right)\approx 0 \tag{16}$$

Equations (14) and (16) interprets that the effect of same amount of change in stiffness $\Delta[K]$ in two finite element models with and without modelling error towards the square of frequency and mode shapes are almost null. Thus, these two modal quantities are least sensitive to modelling error. In this study, low-frequency vibration measurements have been used as output features. The main advantage of using low-frequency vibration measurements is that the low-frequency modes are generally global, and so the vibration sensors may be mounted remotely from the damage site, and fewer sensors can be used.

3.2.1 Variable Screening

Output features should be sensitive enough to the chosen input features. The insignificant input features are screened out, and those are not considered in the model formation. A quantitative evaluation of each parameter's effect on the total model variance can be carried out using analysis of variance (ANOVA) method according to its F-test value.

$$F_A=\frac{\mathrm{SS_R}/k}{\mathrm{SS_E}/(n-k-1)} \tag{17}$$

F_A denotes the F test value of a particular input parameter A. $\mathrm{SS_E}$ and $\mathrm{SS_R}$ are the sum of squares due to the model and the residual (error), respectively. n is the number of samples used in the design procedure. If F_A exceeds the selected criterion value, the input parameter A is said to be significant with respect to the chosen output feature. For sensitivity analysis, the percentage contribution of each input parameter (including the contribution of the interaction terms) to the total model variance can be obtained by summing all the term sum of squares (SS) and then taking each individual SS and dividing it by the total SS and multiplying by 100.

General sensitivity analysis (GSA) may also be used as a fast way to determine which input parameters are important to the output features [52]. A sensitivity coefficient S_i is computed by the first-order derivative of the output feature of interest with respect to each input parameter using finite differencing keeping the input parameter under consideration set to its extreme values, while the values of the remaining input parameters are held at their nominal values. Thus,

$$S_i=\left(\frac{\mathrm{Output_{Hi}}-\mathrm{Output_{Low}}}{\mathrm{Input_{Hi}}-\mathrm{Input_{Low}}}\right)\frac{\mathrm{Input_{Low}}}{\mathrm{Output_{Low}}} \tag{18}$$

Subscripts Hi and Low in Eq. 13 refer to the level at which the input parameter is set.

3.3 Formation of Response Surface Relating Input and Output Features

In this step, the models are formed for responses in terms of input parameters using different design procedures. Numerical models have been used instead of actual experiments in this study. ABAQUS [53] software has been used for finite element analysis. The PYTHON scripts generated using ABAQUS are parameterized to perform multiple runs by varying the structural design parameters to get the corresponding responses. The modified PYTHON script is capable of performing multiple runs taking different set of values (design points) of the above-mentioned structural design parameters.

3.3.1 Model Adequacy Checking

An optimized response surface model is formed by adding or deleting input factors through backward elimination, forward addition or stepwise elimination/addition. It involves

the calculation of the P value (probability value, gives the risk of falsely rejecting a given hypothesis) and Prob. $> F$ value (gives the proportion of time one would expect to get the stated F value if no factor effects are significant). The response surface model constructed should be checked by some criteria such as R^2 (A measure of the amount of variation around the mean explained by the model), R^2_{adj} (A measure of the amount of variation around the mean explained by the model, adjusted for the number of terms in the model. The adjusted R-squared decreases as the number of terms in the model increases if those additional terms do not add value to the model) and R^2_{pred} (A measure of the prediction capability of the response surface model).

$$R^2 = \frac{\text{SS}_\text{R}}{\text{SS}_\text{T}} = 1 - \frac{\text{SS}_\text{E}}{\text{SS}_\text{T}} \qquad \left(0 \le R^2 \le 1\right) \tag{19}$$

$$R^2_{\text{adj}} = 1 - \frac{\text{SS}_\text{E}/(n-k-1)}{\text{SS}_\text{T}/(n-1)} = 1 - \frac{(n-1)}{(n-k-1)}\left(1-R^2\right) \qquad \left(0 \le R^2_{\text{adj}} \le 1\right) \tag{20}$$

$$R^2_{\text{pred}} = 1 - \frac{\text{PRESS}}{\text{SS}_\text{T}} \left(0 \le R^2_{\text{pred}} \le 1\right) \tag{21}$$

where $\text{SS}_\text{T} = \text{SS}_\text{E} + \text{SS}_\text{R}$ is the total sum of square, SS_R and SS_E are regression sum of squares and residual sum of squares, respectively, and PRESS is the predicted residual error sum of squares, which is a measure of how the model fits the samples in the design space. The values of R^2, R^2_{adj} and R^2_{pred} should be close to 1. A difference between R^2_{adj} and R^2_{pred} within 0.2 indicates that the model can be used for further prediction. Another check is adequate precision, which compares the range of the predicted values at the design points with the average prediction error. A value >4 indicates adequate model [54–59]. To check whether the residuals follow normal distribution, either quantitative approaches following Kolmogorov–Smirnov test and Shapiro–Wilk test, or graphical approach (as described in the next paragraph) may be adopted [56–58].

Some plots should also be checked such as normal plot of residuals (indicates whether the residuals follow a normal distribution, in which case, the points will follow a straight line), residuals versus predicted plot (plot of the residuals versus the ascending predicted response values), actual versus predicted plot (a graph of the actual response values versus the predicted response values for the design points used for response surface formation. It helps to detect a value, or group of values, that are not easily predicted by the model), Box–Cox plot (helps to determine the most appropriate power transformation to be applied to response data).

3.4 Identification of Damage

Damage identification using the obtained response surface models is an inverse multi-objective optimization problem, i.e. knowing the measured output features, finding out the input parameters that led to such output values. In this study, damage has been modelled by reducing stiffness of the structure locally. The inverse problem for identifying damage can be described as follows.

$$\left.\begin{array}{l} f_1 = f\ (I_1, I_2, I_3 \ldots) \\ f_2 = f\ (I_1, I_2, I_3 \ldots) \\ f_3 = f\ (I_1, I_2, I_3 \ldots) \\ f_4 = f\ (I_1, I_2, I_3 \ldots) \end{array}\right\} \ f_1, f_2, f_3, f_4 \text{ known}, \longrightarrow I_1, I_2, I_3 \ldots = ? \tag{22}$$

Here, $f_1, f_2, \ldots$ and $I_1, I_2, \ldots$ represent the set of objective functions and input parameters, respectively. For example, let us take the damage identification problem of a simply supported beam (which has been discussed in Sect. 4.1 elaborately). The beam has been divided into ten symmetric sub-structures having section inertias $I_1, I_2, \ldots, I_{10}$. In this case, 30 % damage in sub-structure 3 means 30 % reduction in section inertia value of the sub-structure 3. For this particular example, the problem is like: the dynamic responses (output natural frequencies) of the beam (measured from the damaged beam) are known; the objective is to identify the damage in the structure from this information. In this study, the damage identification results have been verified by comparing them with the actual induced damage in the structure.

For identifying damage, multi-objective optimization algorithm *fgoalattain* from Matlab [60] has been used in the present study. The goal attainment problem is to minimize a slack variable γ as:

$$\min_{x,y} \gamma, \text{ such that } F(x) - w\gamma \le \text{goal}, \quad lb \le x \le ub \tag{23}$$

where $F(x) = \text{abs}\left(\frac{f_{\text{RSM}} - f_{\text{exp}}}{f_{\text{exp}}}\right)$ is a dimensionless objective function with f_{RSM} and f_{exp} denoting the frequencies from the RS model and experiment, respectively. A dimensionless $F(x)$ ensures that different physical quantities can be simultaneously and equally updated. The weight w controls the relative over-attainment and under-attainment of the objectives. In this study, equal weights are given to each $F(x)$; goal is a set of target values of the output features that are to be attained; *lb* and *ub* are the lower and upper bounds of the design space of x.

4 Results and Discussion

In this section, damage identification in three different structures using the procedure explained in Sect. 3 has been dis-

Table 1 Damage scenarios introduced for SDI

Example	Undamaged system	Damage scenario-1	Damage scenario-2	Damage scenario-3
Simply supportedBeam	Section inertia is 3.2552×10^{-4} m^4	20 % reduction in section inertia of substructure-4	30 % reduction in section inertia of substructure-6	30 % reduction in section inertia of substructure-6 plus 20 % reduction in section inertia of substructure-7
Spring mass damper system	Spring stiffness is 10,000 N/m	20 % reduction in spring stiffness of substructure-2	30 % reduction in spring stiffness of substructure-4	20 % reduction in spring stiffness of substructure-1 plus 30 % reduction in spring stiffness of substructure-3
Bridge deck	Section inertia is 144,000 mm^4	20 % reduction in section inertia of substructure-5	20 % reduction in section inertia of substructure-3	30 % reduction in section inertia of substructure-2 plus 40 % reduction in section inertia of substructure-3

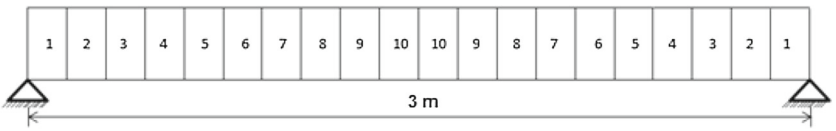

Fig. 5 Dimensions of the simply supported beam

cussed. The objective is to address the comparative ability of different DOE methods of RSM in SDI with the help of these numerical models. Different damage scenarios introduced for SDI in the three examples are collectively shown in Table 1.

4.1 Example I: Simply Supported Beam

4.1.1 Identification of Structure of Interest

A 3 m long simply supported concrete beam having cross section of 0.25 m × 0.25 m has been taken first for SDI. Material properties of the beam are: Young's modulus (E) = 30 GPa, Density (D) = 2,400 kg/m^3, Poisson ratio (P) = 0.2. The beam is divided into 20 identical parts (as shown in Fig. 5) for the damage detection purpose. The beam has been modelled in ABAQUS using C3D8I elements assuring that different section inertia values can be assigned to each of the 20 parts. The Python scripts generated in ABAQUS have been parameterized in such way that they are capable of obtaining the outputs corresponding to different sets of inputs following multiple runs.

4.1.2 Identification of Proper Input and Output Features

Since the beam is having uniform cross section and material property along its length, four parameters, Young's modulus (E), density (D), Poisson ratio (P) and section inertia (I) of substructure number-4 have been taken as initial input parameters. For screening purpose, a 2^k factorial design is adopted having 16 samples. The first four bending frequencies have been taken as responses (output feature) in this case. The bounds (± 1) of each parameter are identically set to be ± 30 % change with respect to the initial values. The percentage contribution to total model variance of each input parameter (including the two factor interaction effects) to the output features has been shown in Fig. 6. From figure, it is evident that chosen output features are highly sensitive to E, I and D, whereas Poisson ratio has almost no effect on output features. However, in most of the real applications, material property (Young's modulus) and mass (density) remain unaltered. Therefore, in the present study, the beam is assumed to be damaged only due to reduction of section inertia (I), i.e. damage has been modelled by reducing the stiffness locally [61]. Furthermore, as modal frequency is a global quantity, damage at two symmetric locations of the symmetric beam will cause same amount of frequency change. Therefore, instead of taking 20 section inertia values, 10 section inertia values ($I_1, I_2, \ldots, I_{10}$) have been taken as input parameter. Here, I_1 denotes the section inertia of substructure-1 consisting of two symmetric parts of the beam part-1 and part-20. Similarly, I_2 denotes the section inertia of substructure-2 consisting of part-2 and part-18 and so on.

To examine the correlation between different output features, correlation coefficient matrix has been formed by the responses obtained from a 1/16th 2^k factorial design using the ten section inertias as input parameter.

$$\rho_{xy} = \begin{bmatrix} 1 & 0.69 & 0.69 & 0.25 \\ 0.69 & 1 & 0.68 & 0.24 \\ 0.69 & 0.68 & 1 & 0.24 \\ 0.25 & 0.24 & 0.24 & 1 \end{bmatrix} \tag{24}$$

where ρ_{xy} is the correlation coefficient matrix having order across and down as f_1, f_2, f_3, f_4. The correlation coefficient matrix shows that the five output features are not highly correlated with each other, and thus, they can be used for model formation.

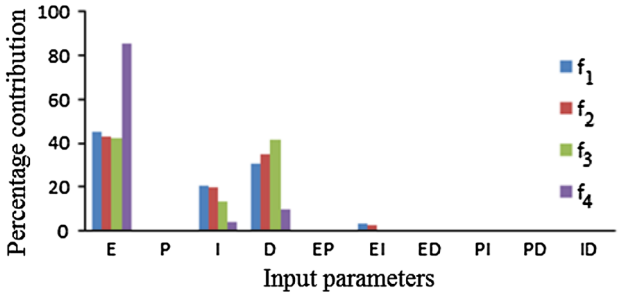

Fig. 6 Parameter screening of the simply supported beam

4.1.3 Formation of Response Surface Relating Input and Output Features

In this section, response surface equations have been formed using different design methods as discussed before. It is noted that, in this study, no replicate samples are used in any of the design methods as there is no experimental error in case of numerical experiments.

4.1.3.1 Formation of Response Surface Using Central Composite Design A MRRV design having 82 training samples comprising of 76 factorial and axial samples plus 6 centre point samples is chosen for analysis. The lower and upper bounds of the factorial part (± 1) are set to $0.7I_0$ and $1.3I_0$ with $\alpha = 1.78$ (practical), where I_0 represents the undamaged section inertia. Second-order response surface models have been developed with some significant interaction terms. A typical actual versus predicted plot for response f_1 and a 3D response plot for response f_4 are shown in Figs. 7 and 8, respectively. A typical response surface model (obtained using central composite design) for f_1(corresponding $R^2 = 0.996$; $R^2_{\text{adj}} = 0.994$; $R^2_{\text{adj}} = 0.984$; Adequate Precision = 119.25) is shown in Eq. 25.

$$
\begin{aligned}
(f_1)^{-3} = {} & 4.00202 \times 10^{-5} + 1.34886 \times 10^{-7} I_1 \\
& - 9.87866 \times 10^{-8} I_2 - 2.85414 \times 10^{-7} I_3 \\
& - 7.94255 \times 10^{-7} I_4 - 1.16127 \times 10^{-6} I_5 \\
& - 1.53641 \times 10^{-6} I_6 - 2.04643 \times 10^{-6} I_7 \\
& - 2.53261 \times 10^{-6} I_8 - 2.41884 \times 10^{-6} I_9 \\
& - 2.59891 \times 10^{-6} I_{10} - 2.41345 \times 10^{-8} I_1 I_3 \\
& + 1.27725 \times 10^{-8} I_4 I_8 - 2.41202 \times 10^{-8} I_6 I_9 \\
& - 4.72066 \times 10^{-8} I_9 I_{10} - 7.40898 \times 10^{-9} I_1^2 \\
& + 8.39661 \times 10^{-9} I_2^2 + 3.79405 \times 10^{-8} I_3^2 \\
& + 7.86034 \times 10^{-8} I_4^2 + 1.26199 \times 10^{-7} I_5^2 \\
& + 1.76083 \times 10^{-7} I_6^2 + 2.23142 \times 10^{-7} I_7^2 \\
& + 2.77319 \times 10^{-7} I_8^2 + 2.89099 \times 10^{-7} I_9^2 \\
& + 2.99815 \times 10^{-7} I_{10}^2 \qquad (25)
\end{aligned}
$$

4.1.3.2 Formation of Response Surface Using 2^k Factorial Design A 1/16th fractional factorial design having 70 samples consisting of 64 factorial samples plus 6 centre point samples is chosen for the analysis. The lower and upper bounds of the factorial part (± 1) are set to $0.7I_0$ and $1.3I_0$, where I_0 represents the undamaged section inertia. First-order response surface models have been developed with some significant interaction terms.

4.1.3.3 Formation of Response Surface Using D-optimal Design An over-determined D-optimal design considering a linear model (with no interaction terms) having total 26 samples consisting of 21 model points plus 5 points to estimate lack of fit has been used employing both Point exchange and Coordinate exchange searches of the design space. The lower and upper bounds (± 1) are set to $0.7I_0$ and I_0, where I_0 represents the undamaged section inertia.

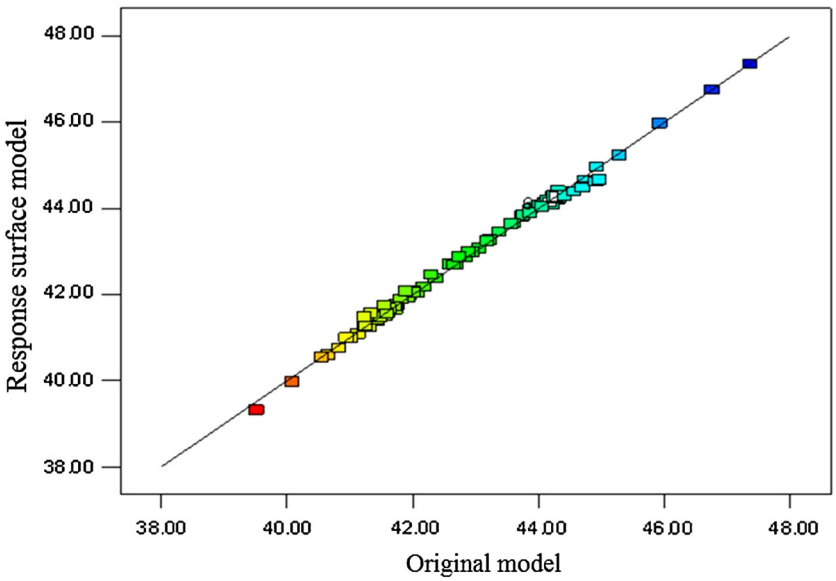

Fig. 7 Typical actual versus predicted plot for response f_1 showing a comparison between the response of original numerical model and response surface model

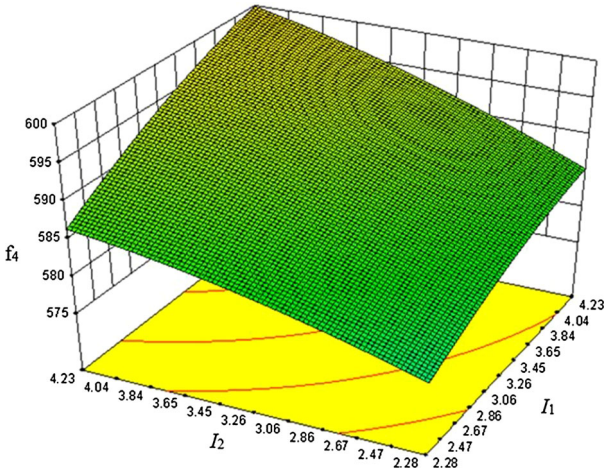

Fig. 8 3D Response surface plot for response f_4 (Hz) with I_1 and I_2 when other input parameters have a constant value of 3.255 mm^4

4.1.3.4 Formation of Response Surface Using Box–Behnken Design A Box–Behnken design having 170 samples including 10 centre point samples has been taken. The lower and upper bounds (± 1) are set to $0.7I_0$ and I_0, where I_0 represents the undamaged section inertia. Second-order response surface models have been developed with some significant interaction terms.

4.1.3.5 Formation of Response Surface Using Taguchi's OA Design A Taguchi's OA Design (L27 array corresponding to 10 input parameters having 3 levels each) having 27 samples has been taken. The three levels chosen are $0.7I_0$, $0.85I_0$ and I_0, where I_0 represents the undamaged section inertia.

4.1.4 Identification of Damage

In this section, the capability to identify damage by using the response surfaces formed by different design methods has been discussed. For this purpose, three damage scenarios including two single damage situations (damage scenario-1: 20 % reduction in section inertia of substructure 4; damage scenario-2: 30 % reduction in section inertia of substructure 6) and one multiple damage situation (damage scenario-3: 30 % reduction in section inertia of substructure 6 plus 20 % reduction in section inertia of substructure 7) have been introduced to the structure. The responses (first four bending frequencies) corresponding to each of the damage conditions are found out first. Then, to judge how the different design methods work for damage detection, the response surfaces formed by different design methods are optimized to find the value of the input parameters (section inertias of ten substructures) which can cause such responses. In Fig. 9 optimization results are shown. Undamaged section inertia of

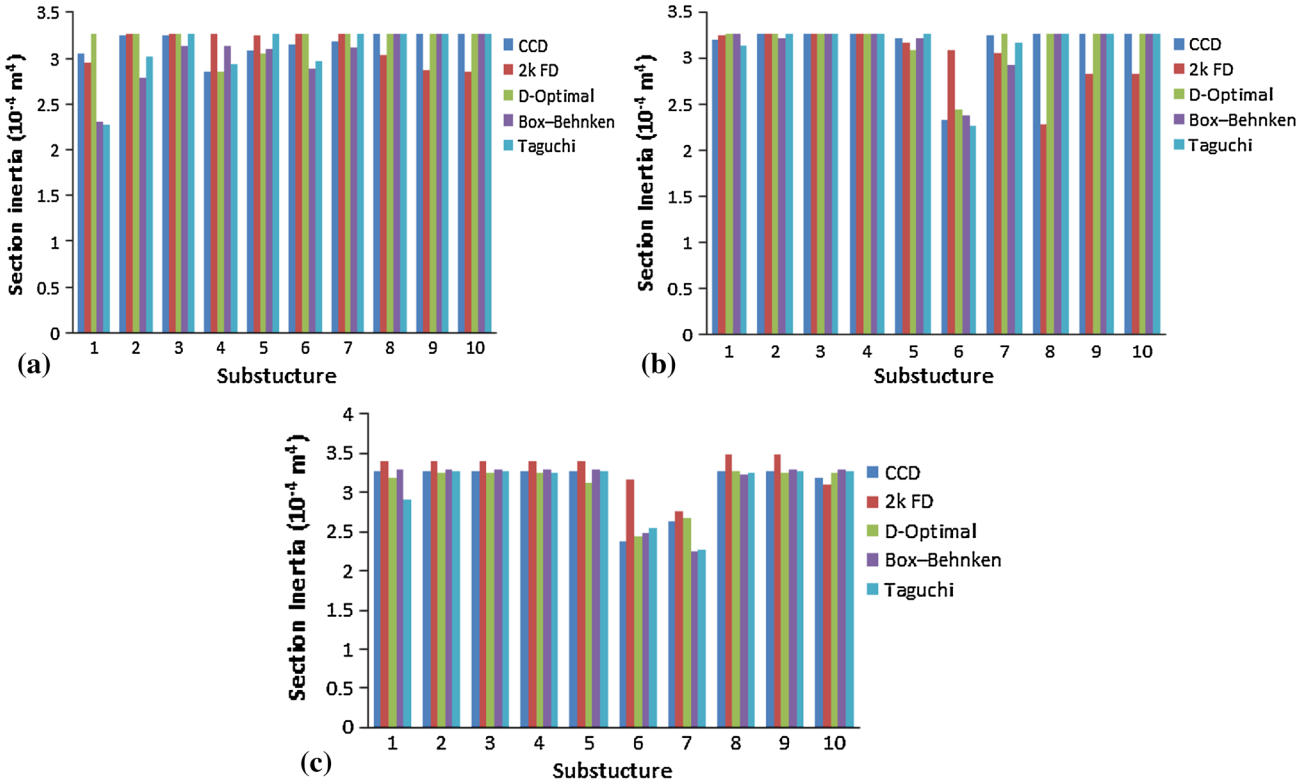

Fig. 9 Damage identification of beam: **a** damage scenario-1, **b** damage scenario-2, **c** damage scenario-3. (Damage scenarios: Table 1)

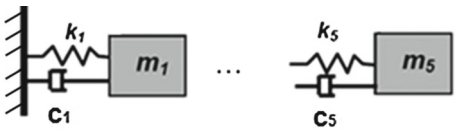

Fig. 10 5DOF spring mass damper system

the beam is 3.2552×10^{-4} m^4. From Fig. 9, it is evident that central composite design and D-optimal design work best for damage detection purpose in the simply supported beam, whereas 2^k factorial design completely fails to identify damage. Box–Behnken design and Taguchi's OA method do not give satisfactory results.

4.2 Example II: Spring Mass Damper System

4.2.1 Identification of Structure of Interest

A 5 degree of freedom system consisting of steel spring, mass and damper has been taken as shown in Fig. 10. Spring stiffness (k), mass (m) and damping (c) of the system are 10,000 N/m, 2 kg, 1 kg/s, respectively, in undamaged condition. The system having five sub-structures consisting of five sets of spring stiffness, mass and damping values has been modelled using ABAQUS. The PYTHON scripts generated in ABAQUS have been parameterized in such a way that they are capable of obtaining the outputs corresponding to different sets of inputs following multiple runs.

4.2.2 Identification of Proper Input and Output Features

In this case, general sensitivity analysis (GSA) has been employed for the purpose of significant input parameter screening. The values of k_2, c_2 and m_2 (input parameters corresponding to substructure 2) are varied ±30 % with respect to their initial values as shown in Table 2. The sensitivity coefficients for each input parameter corresponding to different output responses are shown in Fig. 11. From figure, it is clear that mass and spring stiffness are the significant input parameters when natural frequencies are taken as output features. However, in this case, spring stiffness has been taken as input parameter for damage identification problem assuming

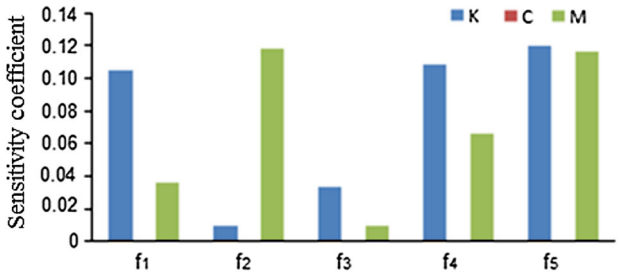

Fig. 11 Parameter screening for spring mass damper system

mass remains unaltered. If damage detection in the dampers is also needed to be carried out, then damped frequencies may be used as output features instead of natural frequencies. In that case, five damping values ($c_1, c_2 \ldots c_5$) can be taken as input parameters along with the spring stiffnesses.

To examine the correlation between different output features, correlation coefficient matrix has been formed by the responses obtained from a 1/2 fractional 2^k factorial design using the five spring stiffness values as input parameter.

$$\rho_{xy} = \begin{bmatrix} 1 & 0.67 & 0.67 & 0.67 & 0.62 \\ 0.67 & 1 & 0.68 & 0.67 & 0.63 \\ 0.67 & 0.68 & 1 & 0.68 & 0.64 \\ 0.67 & 0.67 & 0.68 & 1 & 0.65 \\ 0.62 & 0.63 & 0.64 & 0.65 & 1 \end{bmatrix} \quad (26)$$

where ρ_{xy} is the correlation coefficient matrix having order across and down as f_1, f_2, f_3, f_4, f_5. The correlation coefficient matrix shows that the five output features are not highly correlated with each other, and thus, they can be used for model formation.

4.2.3 Formation of Response Surface Relating Input and Output Features

4.2.3.1 Formation of Response Surface Using Central Composite Design A 1/2 fraction design having 32 training samples comprising of 26 factorial and axial samples plus 6 centre point samples is chosen for analysis. The lower and upper bounds of the factorial part (±1) are set to $0.7k_0$ and k_0 with $\alpha = 2$ (rotatable), where k_0 represents the undamaged

Table 2 GSA input parameter values and corresponding responses

K (N/m)	m (kg)	c (kg/s)	f_1 (Hz)	f_2 (Hz)	f_3 (Hz)	f_4 (Hz)	f_5 (Hz)
13,000	2	1	3.1185	8.6654	13.812	18.410	21.641
7,000	2	1	2.8620	8.5945	13.426	16.843	19.619
10,000	2.6	1	2.9064	8.1919	13.533	16.92	19.344
10,000	1.4	1	3.0005	9.1116	13.65	17.913	21.478
10,000	2	1.3	2.9532	8.6204	13.598	17.457	19.991
10,000	2	0.7	2.9532	8.6204	13.598	17.457	19.991

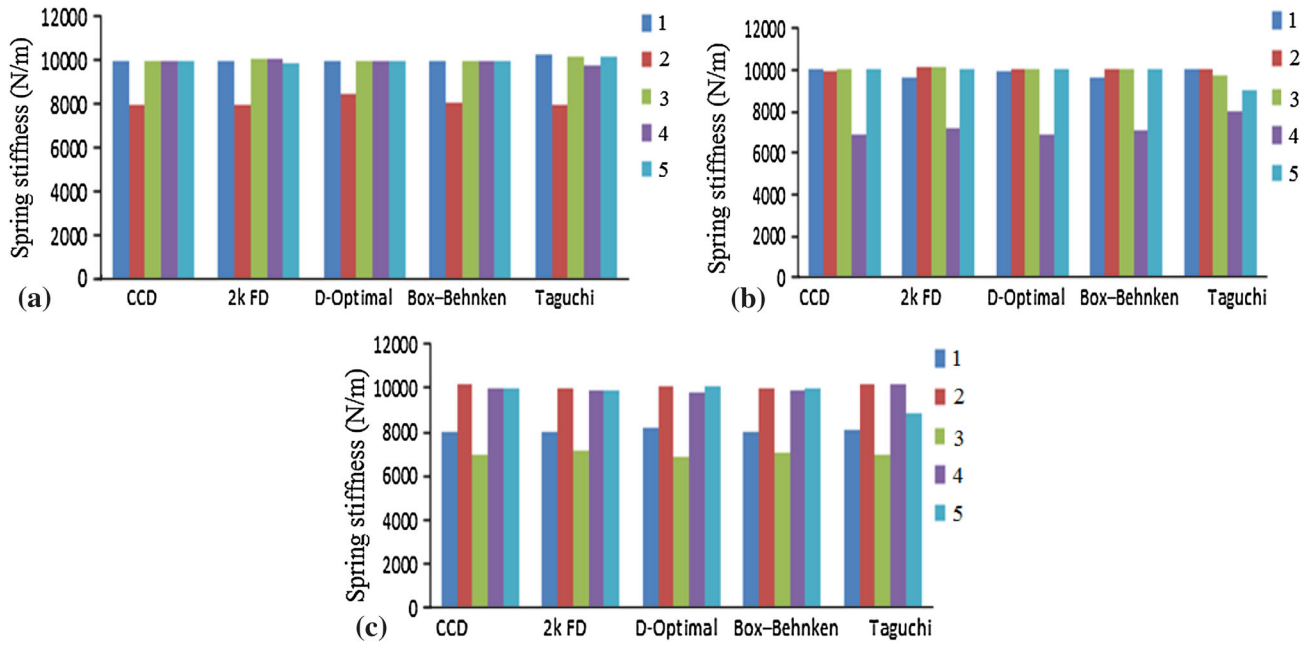

Fig. 12 Damage identification of spring mass damper system: **a** damage scenario-1, **b** damage scenario-2, **c** damage scenario-3. (Damage scenarios: Table 1). Five substructures (1–5) are shown using five different colours

spring stiffness. Second-order response surface models have been developed with some significant interaction terms.

4.2.3.2 Formation of Response Surface Using 2^k Factorial Design A 1/2 fractional factorial design having 21 samples consisting of 16 factorial samples plus 5 centre point samples is chosen for the analysis. The lower and upper bounds of the factorial part (± 1) are set to $0.7k_0$ and k_0, where k_0 represents the undamaged spring stiffness. First-order response surface models have been developed with some significant interaction terms.

4.2.3.3 Formation of Response Surface Using D-optimal Design An over-determined D-optimal design considering a linear model (with no interaction terms) having total 16 samples consisting of 11 model points plus 5 points to estimate lack of fit has been used employing both point exchange and coordinate exchange searches of the design space. The lower and upper bounds (± 1) are set to $0.7k_0$ and k_0, where k_0 represents the undamaged spring stiffness.

4.2.3.4 Formation of Response Surface Using Box–Behnken Design A Box–Behnken design having 46 samples including 6 centre point samples has been taken. The lower and upper bounds (± 1) are set to $0.7k_0$ and k_0, where k_0 represents the undamaged spring stiffness. Second-order response surface models have been developed with some significant interaction terms.

4.2.3.5 Formation of Response Surface Using Taguchi's OA Design A Taguchi's OA Design (L18 array corresponding to 5 input parameters having 3 levels each) having 18 samples has been taken. The three levels chosen are $0.7k_0$, $0.85k_0$ and k_0, where k_0 represents the undamaged spring stiffness.

4.2.4 Identification of Damage

Three damage scenarios including two single damage situations (damage scenario-1: 20 % reduction in spring stiffness of substructure 2; damage scenario-2: 30 % reduction in spring stiffness of substructure 4) and one multiple damage situation (damage scenario-3: 20 % reduction in spring stiffness of substructure 1 plus 30 % reduction in spring stiffness of substructure 3) have been introduced to the system. In Fig. 12 damage detection results have been shown for different design methods. Undamaged spring stiffness is 10,000 N/m. Fig. 12 shows that all the design methods can perfectly identify damage and its severity except Taguchi's OA method.

4.3 Example III: FRP Composite Bridge Deck

4.3.1 Identification of Structure of Interest

A fibre reinforced polymer (FRP) bridge deck with panel of dimension 3 m × 1 m having one way rib core cross section has been taken as shown in Fig. 13. The ribs are considered to be oriented in the transverse direction only.

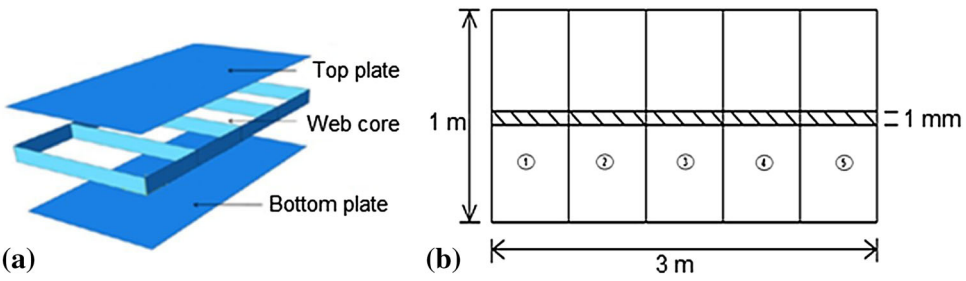

Fig. 13 (**a**) Components of the composite bridge deck (**b**) Substructures of the bottom plate

The panel is simply supported in one edge and having roller support in the opposite edge while the other edges are taken as free. The top plate and bottom plate consist of three plies (0°/90°/0°) having thicknesses 28 and 40 mm each, respectively. The web core consists of two plies (45°/−45°) having thickness 28 mm each. Material properties of the GFRP used are: mass density(D) = 1,828 kg/m^3; Elastic properties: E_1 = 23 GPa; E_2 = 18 GPa; G_{12} = 9 GPa; G_{13} = 9 GPa; G_{23} = 4.5 GPa; Poisson ratio (P) = 0.25 [62]. Different structural components of bridge deck system such as top face sheet, bottom face sheet and web core have been modelled using conventional shell elements (i.e. S4R: Conventional Stress/Displacement 3D Shell, 4-node, Reduced Integration) having three displacements and three rotational degrees of freedom at each node in ABAQUS. The shape of the shell elements are considered to be quadrilateral having linear element geometry. In mesh module, the top and bottom face plates are meshed by 80 by 80 divisions and the rib core is meshed with a global seed size of 80 mm. The mesh sizes have been finalized using convergent studies of mesh division. The interaction between the common nodes of the individual components is defined by using tie elements to avoid the slip between two adjacent surfaces. The Python scripts generated in ABAQUS have been parameterized in such way that they are capable of obtaining the outputs corresponding to different sets of inputs multiple runs.

4.3.2 Identification of Proper Input and Output Features

For the composite bridge deck, eight parameters, elastic moduluses (E_1, E_2, G_{12}, G_{13}, G_{23}), density (D), Poisson ratio (P) and section inertia (I) of substructure-2 of the bottom plate are taken as input parameters for screening as flexure cracks are most likely to appear in the bottom plate for this structure. A D-optimal design having 14 samples is adopted for screening purpose. The two levels of each input parameter are identically set to be ±30 % change with respect to their initial values. The first four bending frequencies are taken as responses (output feature). The percentage contribution of each input parameter (including the important two factor interaction effects) to the output features have been

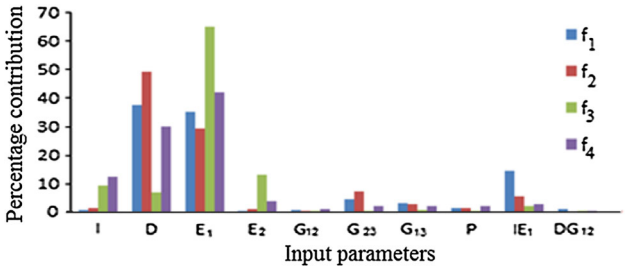

Fig. 14 Parameter screening of the composite bridge deck

shown in Fig. 14. From figure, it is evident that chosen output features are highly sensitive to all the input parameters. However, in the present study, the composite bridge deck is assumed to be damaged only due to reduction in section inertia (I) as material nonlinearity is not present here and density does not change practically for most of the engineering applications. Thus, five section inertia values of sections having unit width corresponding to five substructures ($I_1, I_2, \ldots, I_5$) are taken as input parameters as shown in Fig. 13b.

To examine the correlation between different output features, correlation coefficient matrix has been formed by the responses obtained from a 1/2 fraction 2^k factorial design using the five section inertias as input parameter.

$$\rho_{xy} = \begin{bmatrix} 1 & 0.8 & 0.48 & 0.8 \\ 0.8 & 1 & 0.52 & 0.75 \\ 0.48 & 0.52 & 1 & 0.68 \\ 0.8 & 0.75 & 0.68 & 1 \end{bmatrix} \tag{27}$$

where ρ_{xy} is the correlation coefficient matrix having order across and down as f_1, f_2, f_3, f_4. The correlation coefficient matrix shows that the five output features are not highly correlated with each other, and thus, they can be used for model formation.

4.3.3 Formation of Response Surface Relating Input and Output Features

4.3.3.1 Formation of Response Surface Using Central Composite Design A 1/2 fraction design having 32 training samples comprising of 26 factorial and axial samples plus 6

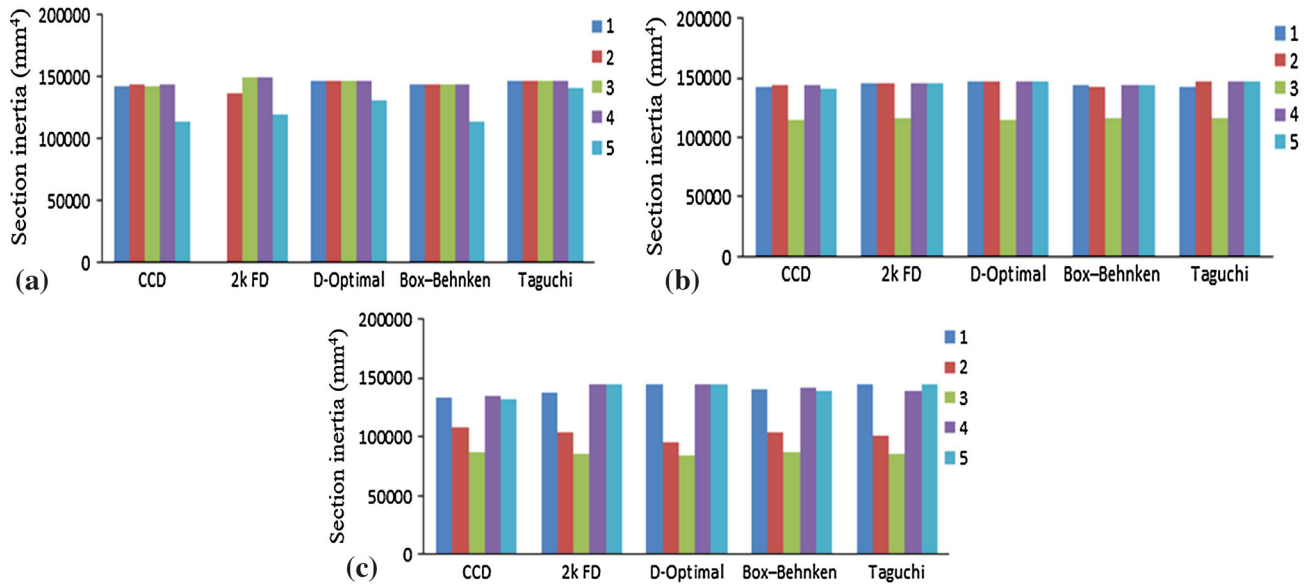

Fig. 15 Damage identification of the composite bridge deck: **a** damage scenario-1, **b** damage scenario-2, **c** damage scenario-3. (Damage scenarios: Table 1). Five substructures (1–5) are shown using *five different colours*

centre point samples is chosen for analysis. The lower and upper bounds of the factorial part (± 1) are set to $0.6I_0$ and I_0 with $\alpha = 2$ (rotatable), where I_0 ($= 144{,}000\,\text{mm}^4$) represents the undamaged section inertia of a strip of the bottom plate having 1 mm width. Second-order response surface models have been developed with some significant interaction terms.

4.3.3.2 Formation of Response Surface Using 2^k Factorial Design A 1/2 fractional factorial design having 21 samples consisting of 16 factorial samples plus 5 centre point samples is chosen for the analysis. The lower and upper bounds of the factorial part (± 1) are set to $0.6I_0$ and I_0, where I_0 represents the undamaged section inertia of a strip of the bottom plate having 1 mm width. First-order response surface models have been developed for this purpose.

4.3.3.3 Formation of Response Surface Using D-optimal Design An over-determined D-optimal design considering a linear model (with no interaction terms) having total 16 samples consisting of 11 model points plus 5 points to estimate lack of fit has been used employing both Point exchange and coordinate exchange searches of the design space. The lower and upper bounds (± 1) are set to $0.6I_0$ and I_0, where I_0 represents the undamaged section inertia of a strip of the bottom plate having 1 mm width.

4.3.3.4 Formation of Response Surface Using Box–Behnken Design A Box–Behnken design having 46 samples including 6 centre point samples has been taken. The lower and upper bounds (± 1) are set to $0.6I_0$ and I_0, where I_0 represents the undamaged section inertia of a strip of the bottom plate having 1 mm width. Second-order response surface models have been developed with some significant interaction terms.

4.3.3.5 Formation of Response Surface Using Taguchi's OA Design A Taguchi's OA Design (L18 array corresponding to 5 input parameters having 3 levels each) having 18 samples has been taken. The three levels chosen are $0.6I_0$, $0.8I_0$ and I_0, where I_0 represents the undamaged section inertia of a strip of the bottom plate having 1 mm width.

4.3.4 Identification of Damage

Three damage scenarios including two single damage situations (damage scenario-1: 20 % reduction in section inertia of substructure 5; damage scenario-2: 20 % reduction in section inertia of substructure 3) and one multiple damage situation (damage scenario-3: 30 % reduction in section inertia of substructure 2 plus 40 % reduction in section inertia of substructure 3) have been introduced to the system. Section inertia of healthy system is $144{,}000\,\text{mm}^4$. In Fig. 15, damage detection results have been shown for different design methods. Figure shows that 2^k factorial design fails to identify damage for the damage scenario-1, and though Taguchi's OA design identifies all the damage locations properly, but it fails to predict the severity of damage for damage scenario-1. All other design methods work satisfactorily for the detection of damage in the composite bridge deck structure.

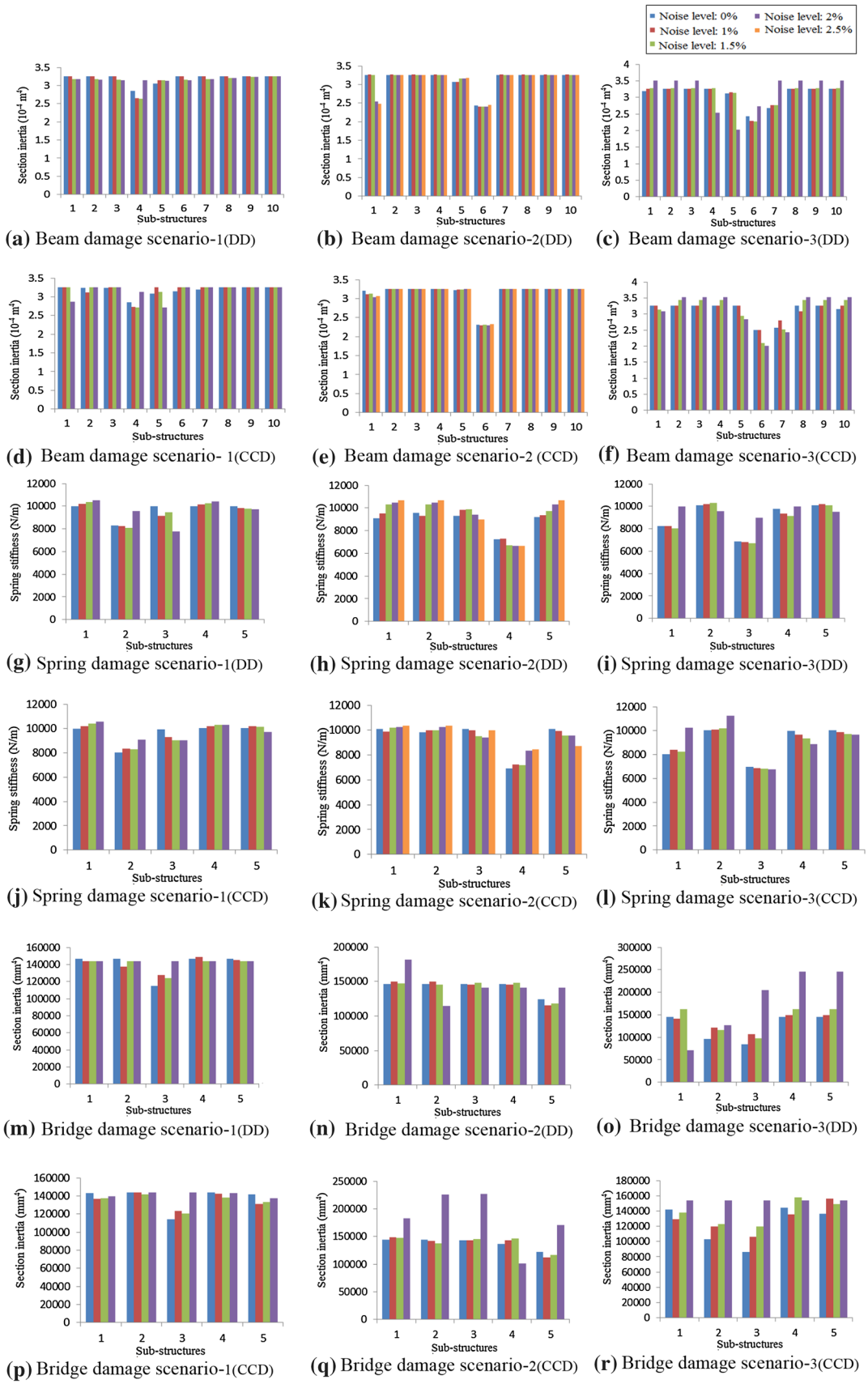

Fig. 16 Effect of noise on SDI based on RSM (damage scenarios: Table 1)

Table 3 Relative damage identification capability of different design methods

Example	Number of input parameters	Number of output parameters	Design method used	Number of design points	Capability in damage identification
Simply supported beam	10	4	CCD (MRRV)	82	Satisfactory
			2^k FD (1/16th fraction)	70	Failed
			D-optimal	26	Satisfactory
			Box–Behnken	170	Failed
			Taguchi's OA	27	Failed
Spring mass damper system	5	5	CCD (1/2 fraction)	32	Satisfactory
			2^k FD (1/2 fraction)	21	Satisfactory
			D-optimal	16	Satisfactory
			Box–Behnken	46	Satisfactory
			Taguchi's OA	18	Failed
Composite bridge deck	5	4	CCD (1/2 fraction)	32	Satisfactory
			2^k FD (1/2 fraction)	21	Failed
			D-optimal	16	Satisfactory
			Box–Behnken	46	Satisfactory
			Taguchi's OA	18	Failed

5 Performance of RSM-Based Damage Identification Techniques Under the Effect of Noise

Effect of inevitable external noise in damage identification problems is very crucial. Moreover, the field vibration measurements may suffer from certain unavoidable errors, which make the damage identification process even more difficult. To judge the performance of central composite design (CCD) and D-optimal design (DD), which are best suited for structural damage identification (as discussed in Sect. 4), simulated noise has been introduced to the natural frequencies for mimicking the actual field condition as follows

$$f = f_{\text{original}} \times (1 + p \times \text{randn}) \tag{28}$$

where f_{original} and f represent the set of numerically obtained natural frequencies and the randomly varied natural frequencies, respectively. p is the percentage of noise. *randn* is a Matlab function, which generates random numbers drawn from a normal distribution having zero mean and unit standard deviation. Four noise levels (1, 1.5, 2 and 2.5 %) were introduced to each of the three structures (simply supported beam, spring mass damper system and FRP composite bridge deck) for the aforementioned two DOE methods. Three different damage scenarios for each of the three structures have been checked to study the influence of noise in SDI as shown in Table 2. Damage identification results using different levels of noisy data are shown in Fig. 16. Results show that almost in all the cases the RSM-based damage identification methods can work satisfactorily up to a simulated noise level of 1.5 % for both CCD and DD.

6 Conclusions

This research explores the comparative capability of different DOE methods used for RSM in the realm of damage identification of engineering structures from the perspective of accuracy and computational efficiency. Subsequently, their performance in SDI under the influence of inevitable noise has also been addressed in this paper. Three numerical examples have been used for the purpose of this comparative study. In the present research, response surface metamodels have been formed by taking the minimum possible number of samples in all the cases. If the sample size of different DOE methods is increased, the accuracy of SDI is expected to improve, but at the cost of higher computational effort. The salient points which come out from this research are summarized below:

1. SDI using RSM demands for very perfect fitting of the response surface models, as an inverse method using multi-objective optimization is involved in the damage identification process. A concise report on the comparative ability of different DOE methods in SDI is presented in Table 3. 2^k factorial design and Taguchi's OA design cannot perform well in the realm of damage detection because of their poor prediction capability. The performance of Box–Behnken design is also not satisfactory when the number of input parameters is more.
2. D-optimal design and central composite design give the best result in SDI, as in both the methods, the chosen design points can capture the overall design space accurately. D-optimal design requires much lesser number of samples for metamodel formation compared with the

other DOE methods ensuring high computational efficiency.

3. Size of the design space while forming the response surface metamodel should be as small as possible with accordance to the expected range of damage to maximize the density of design points over the design domain. For example, if the expected damage is around 15 % reduction of section inertia (I), then the range of input parameters can be taken as $0.7I$ to I, instead of unnecessarily expanding the design space.
4. For parameter screening purpose, all the methods used, i.e. 2^k factorial design, D-optimal design and General sensitivity method, give satisfactory results.
5. Central composite design and D-optimal design are found to be working satisfactorily in damage identification up to a level of 1.5 % simulated noise, demonstrating the capability of RSM-based damage identification method to work satisfactorily in experimental/field condition.
6. Damage location as well as extent of damage can be more accurately identified if the number of substructures is increased, but at the same time, more number of samples will be needed for response surface formation, resulting more computational efforts. When large number of input parameters is involved in a multi-objective optimization, the chances of getting false/poor results also increase in the inverse optimization process. Rather, an iterative process can be tried for this purpose. For example, in case of the simply supported beam, we can first divide it into 20 substructures. Say, damage is identified in substructure 4. Then in the second step, the substructure-4 can be divided into some finite number of substructures again, keeping all other substructures in undamaged state and the same damage identification strategy can be implemented on the new substructures of substructure-4 and so on. In this way, the exact location of the damage and damage intensity can be obtained. The success of this method will depend on the sensitivity of the input parameters to the selected output features.

The research presented in this paper can be useful for further investigation in RSM-based damage identification method for its implementation in more complex structures as well as field application. Furthermore, the present work can serve as an important reference for future researches in many other fields of science and engineering involving response surface-based multi-objective optimization for choosing the appropriate DOE method.

Acknowledgments The authors would like to acknowledge the financial support received from MHRD, India, during the period of this research work.

References

1. Farrar, C.R.; Worden, K.: An introduction to structural health monitoring. Philos. Trans. R. Soc. A **365**, 303–315 (2007)
2. Doebling, S.W.; Farrar, C.R.; Prime, M.B.; Shevitz, D.W.: Damage Identification and Health Monitoring of Structural and Mechanical Systems from Changes in Their Vibration Characteristics: A Literature Review. LANL report (LA-13070-MS) (1996)
3. Fan, W.; Qiao, P.: Vibration-based damage identification methods: a review and comparative study. Struct. Health Monit. **10**(1), 83–29 (2011)
4. Fritzen, C.P.: Vibration-based structural health monitoring—concepts and applications. Key Eng. Mater. **293–294**, 3–20 (2005)
5. Huth, O.; Feltrin, G.; Maeck, J.; Kilic, N.; Motavalli, M.: Damage identification using modal data: Experiences on a prestressed concrete bridge. J. Struct. Eng. **131**, 1898–1910 (2005)
6. Perera, R.; Fang, S.E.; Ruiz, A.: Application of particle swarm optimization and genetic algorithms to multiobjective damage identification inverse problems with modelling errors. Meccanica **45**(5), 723–734 (2010)
7. Dash, K.A.; Parhi, D.R.: Analysis of an intelligent hybrid system for fault diagnosis in cracked structure. Arab. J. Sci. Eng. **39**(2), 1337–1357 (2013)
8. Sehgal, S.; Kumar, H.: Damage detection using Derringer's function based weighted model updating method. In: Structural Health Monitoring. Conference Proceedings of the Society for Experimental Mechanics Series vol. 5, pp. 241–253 (2014)
9. Burczynski, T.; Beluch, W.: The identification of cracks using boundary elements and evolutionary algorithms. Eng. Anal. Boundary Elem. **25**(4), 313–322 (2001)
10. Bicanic, N.; Chen, H.P.: Damage identification in framed structures using natural frequencies. Int. J. Numer. Methods Eng. **40**(23), 4451–4468 (1997)
11. Pandey, A.K.; Biswas, M.; Samman, M.M.: Damage detection from changes in curvature mode shapes. J. Sound Vib. **145**, 331–332 (1991)
12. Zimmerman, D.C.; Kaouk, M.: Structural damage detection using a minimum rank update theory. J. Vib. Acoust. **116**, 222–231 (1994)
13. Pandey, A.K.; Biswas, M.: Damage detection in structures using changes in flexibility. J. Sound Vib. **169**, 3–17 (1994)
14. Stubbs, N.; Kim, J.T.: Field verification of a non-destructive damage localization and severity estimation algorithm. In: Texas A and M University Report, New Mexico State University (1994)
15. Banan, M.R.; Banan, M.R.; Hjelmstad, K.D.: Parameter estimation of structures from static response I: computational aspects. J. Struct. Eng. **120**(11), 3243–3258 (1994)
16. Sanayei, M.; Saletnik, M.J.: Parameter estimation of structures from static strain measurements II: formulation. J. Struct. Eng. **122**(5), 555–562 (1996)
17. Mark, W.; George, D.: A Brief Description of NDT Techniques. Insight NDT Equipment Ltd (2003)
18. McCann, D.M.; Forde, M.C.: Review of NDT methods in the assessment of concrete and masonry structures. NDT E Int. **34**, 71–84 (2001)
19. Lim, Y.Y.; Bhalla, S.; Soh, C.K.: Structural identification and damage diagnosis using self-sensing piezo-impedance transducers. Smart Mater. Struct. **15**(3), 987–995 (2006)
20. Naskar, S.; Bhalla, S.: Experimental investigations of metal wire based EMI technique for steel structures. In: Seventh ISSS International Conference on Smart Materials Structures and Systems ISSS (2014)
21. Chang, C.C.; Chen, L.W.: Detection of the location and size of cracks in the multiple cracked beam by spatial wavelet based approach. Mech. Syst. Signal Process. **19**, 139–155 (2005)

22. Hein, H.; Feklistova, L.: Computationally efficient delamination detection in composite beams using Haar wavelets. Mech. Syst. Signal Process. **25**(6), 2257–2270 (2011)
23. Wu, N.; Wang, Q.: Experimental studies on damage detection of beam structures with wavelet transform. Int. J. Eng. Sci. **49**, 253–261 (2011)
24. Feklistova, L.; Hein, H.: Crack identification in vibrating beams using Haar wavelets and neural networks. In: Applied mechanics and materials: 2013 International Conference on Recent Trends in Materials and Mechanical Engineering, Singapore, 21–23 September (2013)
25. Katunin, A.; Przystałka, P.: Damage assessment in composite plates using fractional wavelet transform of modal shapes with optimized selection of spatial wavelets. Eng. Appl. Artif. Intell. **30**, 73–85 (2014)
26. Katunin, A.; Przystałka, P.: Meta-optimization method for wavelet-based damage identification in composite structures. FedCSIS **2**, 429–438 (2014). doi:10.15439/2014F268
27. Fu, Y.Z.; Lu, Z.R.; Liu, J.K.: Damage identification in plates using finite element model updating in time domain. J. Sound Vib. **332**(26), 7018–7032 (2013)
28. Moaveni, B.; He, X.; Conte, J.P.; Callafon, R.A.D.: Damage identification of a composite beam using finite element model updating. Comput. Aided Civil Infrastruct. Eng. **23**(5), 339–359 (2008)
29. Box, G.E.P.; Wilson, K.B.: On the experimental attainment of optimum conditions. J. R. Stat. Soc. Ser. B **13**, 1–45 (1951)
30. Myers, R.H.; Montgomery, D.C.: Response Surface Methodology: Process and Product Optimization Using Designed Experiments, 2nd edn. Wiley, New York (2002)
31. Khuri, A.I., Mukhopadhyay, S.: Response surface methodology. Wiley Interdiscip. Rev. Comput. Stat. **2**(2), 128–149 (2010). doi:10.1002/wics.73
32. Noordin, M.Y.; Venkatesh, V.C.; Sharif, S.; Elting, S.; Abdullah, A.: Application of response surface methodology in describing the performance of coated carbide tools when turning AISI 1045 steel. J. Mater. Process. Technol. **145**, 46–58 (2004)
33. Carpenter, W.C.: Effect of design selection on response surface performance. NASA Contractor Report 4520 (1993)
34. Lee, S.H.; Kwak, B.M.: Response surface augmented moment method for efficient reliability analysis. Struct. Saf. **28**, 261–72 (2006)
35. Faravelli, L.: Response surface approach of reliability analysis. J. Eng. Mech. **115**(12), 2763–2781 (1989)
36. Senthilkumar, N.; Tamizharasan, T.; Gobikannan, S.: Application of response surface methodology and firefly algorithm for optimizing multiple responses in turning AISI 1045 Steel. Arab. J. Sci. Eng. doi:10.1007/s13369-014-1320-3 (2014)
37. Subramanian, M.; Sakthivel, M.; Sudhakaran, R.: Modeling and analysis of surface roughness of AL7075-T6 in end milling process using response surface methodology. Arab. J. Sci. Eng. **29**(10), 7299–7313 (2014)
38. Huh, J.; Haldar, A.: Stochastic finite-element-based seismic risk of nonlinear structures. J. Struct. Eng. **127**(3), 323–329 (2001)
39. Gao, X.; Low, T.S.; Chen, S.; Liu, Z.: Structural Robust Design for Torque Optimization of BLDC Spindle Motor Using Response Surface Methodology. IEEE Trans. Magn. **37**(4), 2814–2817 (2001)
40. Guo, Q.T.; Zhang, L.M.: Finite element model updating based on response surface methodology. In: Proceedings of 22nd International Modal Analysis Conference (Dearborn, MI) (2004)
41. Hemez, F.M.; Wilson, A.C.; Doebling, S.W.: Design of computer experiments for improving an impact test simulation. In: 19th International Modal Analysis Conference, Kissimmee, FL (2001)
42. Cundy, A.L.; Schultze, J.F.; Hemez, F.M.; Doebling, S.W.; Bingham, D.: Variable screening methods in metamodel design for a large structural dynamics simulation. In: 20th International Modal Analysis Conference, Los Angeles, CA (2002)
43. Shinn, R.; Hemez, F.M.; Doebling, S.W.: Estimating the error in simulation prediction over the design space. In: 44th AIAA/ASME/ASCE/AHS Structures, Structural Dynamics, and Materials Conference, Norfolk, VA (2003)
44. Ren, W.X.; Chen, H.B.: Finite element model updating in structural dynamics by using response surface method. Eng. Struct. **32**(8), 2455–2465 (2008)
45. Cundy, A.L.: Use of Response Surface Metamodels in Damage Identification of Dynamic Structures, Master thesis. Virginia Polytechnic Institute and State University (2002)
46. Cho, T.: Prediction of cyclic freeze–thaw damage in concrete structures based on response surface method. Constr. Build. Mater. **21**, 2031–40 (2007)
47. Fang, S.E.; Perera, R.: A response surface based damage identification technique. Smart Mater. Struct. **18**, 065009 (2009)
48. Casciati, S.: Response surface models to detect and localize distributed cracks in a complex continuum. J. Eng. Mech. **136**(9), 1131–1142 (2010)
49. Unal, R.; Lepscht, R.A.; McMillin, M.L.: Response surface model building and multidisciplinary optimization using D-optimal designs. In: Annual AIAA/ NASA/ISSMO Symposium on Multidisciplinary Analysis and Optimization, Seventh, St. Louis, MO, USA, pp. 10–31 (1998)
50. Michael, J.B.; Norman, R.D.: On minimum-point second-order designs. Technometrics **16**(4), 613–616 (1974)
51. Mukhopadhyay, T.; Dey, T.K.; Dey, S.; Chakrabarti, A.: Optimization of fiber reinforced polymer web core bridge deck—a hybrid approach. Struct. Eng. Int. (2015) (in Press)
52. Hamby, D.M.: A review of techniques for parameter sensitivity analysis of environmental models. Environ. Monit. Assess. **32**, 135–154 (1994)
53. ABAQUS CAE 6.8. Dassault Systèmes Simulia Corp. (2008)
54. Elliott, A.C.; Woodward, W.A.: Statistical Analysis Quick Reference Guidebook with SPSS Examples. 1st ed. Sage, London (2007)
55. Online e-book: Engineering Statistics Handbook, Publisher: NIST/SEMATECH (2003)
56. Peat, J.; Barton, B.: Medical Statistics: A Guide to Data Analysis and Critical Appraisal. Blackwell, Oxford (2005)
57. Oztuna, D.; Elhan, A.H.; Tuccar, E.: Investigation of four different normality tests in terms of type 1 error rate and power under different distributions. Turkish J. Med. Sci. **36**(3), 171–6 (2006)
58. Thode, H.C. Jr.: Testing for Normality. Marcel Dekker, New York. Inc. ISBN 0-8247-9613-6 (2002)
59. Field, A.: Discovering Statistics Using SPSS, 3rd ed,. SAGE, London (2009)
60. Matlab Version 7.12.0.635 (R2011a), MathWorks Inc (2011)
61. Friswell, M.I.; Penny, J.E.T.: Crack modeling for structural health monitoring. Struct. Health Monit. **1**(2), 0139–148 (2002)
62. Dey, T.K.; Srivastava, I.; Khandelwal, P.R.; Sharma, K.U.; Chakrabarti, A.: Optimum design of FRP rib core bridge deck. Compos. Part B **45**(1), 930–938 (2013)